



Published in final edited form as:

J Am Chem Soc. 2018 August 01; 140(30): 9357–9360. doi:10.1021/jacs.8b04751.

Conformationally Regulated Peptide Bond Cleavage in Bradykinin

Daniel R. Fuller[†], Christopher R. Conant[†], Tarick J. El-Baba[†], Christopher J. Brown[†], Daniel W. Woodall[†], David H. Russell[‡], and David E. Clemmer^{*†}

[†]Department of Chemistry, Indiana University, Bloomington, Indiana 47405, United States

[‡]Department of Chemistry, Texas A&M University, College Station, Texas 77842, United States

Abstract

Ion mobility and mass spectrometry techniques are used to investigate the stabilities of different conformations of bradykinin (BK, Arg¹-Pro²-Pro³-Gly⁴-Phe⁵-Ser⁶-Pro⁷-Phe⁸-Arg⁹). At elevated solution temperatures, we observe a slow protonation reaction, i.e., [BK+2H]²⁺+H⁺ → [BK+3H]³⁺, that is regulated by *trans* → *cis* isomerization of Arg¹-Pro², resulting in the Arg¹-*Cis*-Pro²-*cis*-Pro³-Gly⁴-Phe⁵-Ser⁶-*cis*-Pro⁷-Phe⁸-Arg⁹ (all-*cis*) configuration. Once formed, the all-*cis* [BK+3H]³⁺ spontaneously cleaves the bond between Pro²-Pro³ with perfect specificity, a bond that is biologically resistant to cleavage by any human enzyme. Temperature-dependent kinetics studies reveal details about the intrinsic peptide processing mechanism. We propose that nonenzymatic cleavage at Pro²-Pro³ occurs through multiple intermediates and is regulated by *trans* → *cis* isomerization of Arg¹-Pro². From this mechanism, we can extract transition state thermochemistry: $G^\ddagger = 94.8 \pm 0.2 \text{ kJ}\cdot\text{mol}^{-1}$, $H^\ddagger = 79.8 \pm 0.2 \text{ kJ}\cdot\text{mol}^{-1}$, and $S^\ddagger = -50.4 \pm 1.7 \text{ J}\cdot\text{mol}^{-1}\cdot\text{K}^{-1}$ for the *trans* → *cis* protonation event; and, $G^\ddagger = 94.1 \pm 9.2 \text{ kJ}\cdot\text{mol}^{-1}$, $\rightarrow H^\ddagger = 107.3 \pm 9.2 \text{ kJ}\cdot\text{mol}^{-1}$, and $\rightarrow S^\ddagger = 44.4 \pm 5.1 \text{ J}\cdot\text{mol}^{-1}\cdot\text{K}^{-1}$ for bond cleavage. Biological resistance to the most favored intrinsic processing pathway prevents formation of Pro³-Gly⁴-Phe⁵-Ser⁶-*cis*-Pro⁷-Phe⁸-Arg⁹ that is approximately an order of magnitude more antigenic than BK.

Graphical Abstract

*Corresponding Author: clemmer@indiana.edu.

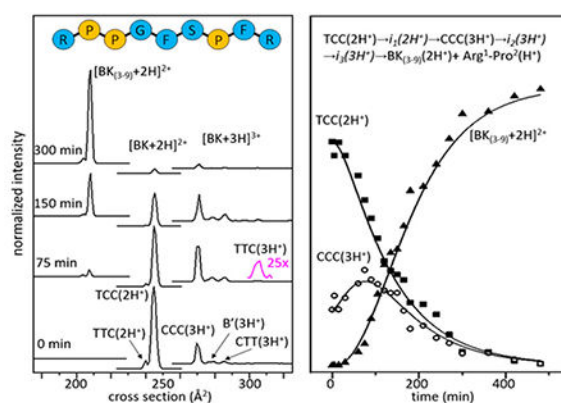
ASSOCIATED CONTENT

Supporting Information

The Supporting Information is available free of charge on the ACS Publications website at DOI: 10.1021/jacs.8b04751.

Experimental details, sequence determination of [BK(3–9)+2H]²⁺, *cis/trans* assignments of [BK+2H]²⁺ conformations, kinetics data at other temperatures, BK dissociation in other solutions, list of trial models tested, acetic acid dependence plot, and Arrhenius plot (PDF)

The authors declare no competing financial interest.



While investigating the solution structure of bradykinin (BK, Arg¹-Pro²-Pro³-Gly⁴-Phe⁵-Ser⁶-Pro⁷-Phe⁸-Arg⁹) by a new hybrid temperature-controlled electrospray ionization (T-ESI),¹⁻³ ion mobility spectrometry (IMS) and mass spectrometry (MS) technique,⁴ we find evidence for a conformationally regulated proton-transfer event that spontaneously cleaves the Pro²-Pro³ peptide bond with perfect specificity, leading to the smaller, seven-residue BK₍₃₋₉₎ species. This is a remarkable finding. In their comprehensive 1995 review, “Proline motifs in peptides and their biological processing,” Scharpe and co-workers emphasize, “the bond between two Pro residues, when not positioned at the N-terminus, possess a high degree of resistance to any human proteolytic enzyme.”⁵ Resistance arises because dipeptidyl peptidase IV (DPP-IV) cannot directly cleave Pro-Pro bonds.⁵ Instead, biological processing of N-terminal residues of BK is initiated by aminopeptidase P elimination of Arg¹, and the remaining BK₍₂₋₉₎ sequence is then susceptible to DPP-IV processing.⁵ Below, we show that the most difficult bond to cleave enzymatically is intrinsically not only most facile, but uniquely specific and cleaved with 100% efficiency in the absence of enzymes. A comparison of our mechanism for spontaneous cleavage of free BK in solution with proposed enzymatic mechanisms suggests that the difference lies in the *cis-trans* configuration of Arg¹-Pro². The ability to follow detailed configurational changes that lead to peptide processing in the absence of enzymes provides a new means of understanding the role of peptidases and the importance of conformational changes in biological processing.

BK possesses hypotensive activity⁶ and is involved in numerous physiological conditions, including pain and inflammation.⁷⁻⁹ Structural studies show that conformations of BK depend upon its environment.¹⁰ C-terminal Ser⁶-Arg⁹ forms a stable turn in polar solvents.¹¹ However, each proline can adopt either *cis* or *trans* configurations leading to multiple structures that are difficult to characterize,¹² and some to conclude that the N-terminal region of BK is unstructured.^{13,14}

Figure 1 shows typical mass spectra recorded using our T-ESI-IMS-MS^{4,15,16} technique, acquired upon incubating BK in an ethanol, 0.5% acetic acid solution (for acid concentration dependence, see Supporting Information) at 65 °C. Similar results are found when BK is incubated in water, methanol and propanol (see Supporting Information). Initially, two peaks are observed in the mass spectrum at $m/z = 531$ and 354 , correspond to intact [BK+2H]²⁺ and [BK+3H]³⁺, respectively. As time progresses, the abundance of [BK+2H]²⁺ decreases

and $[\text{BK}+3\text{H}]^{3+}$ increases. By ~ 75 min, two new peaks, at $m/z = 404$ and 254 are observed. These peaks correspond to a complementary pair of fragments formed in solution and are assigned as the seven-residue $[\text{BK}_{(3,9)}+2\text{H}]^{2+}$ peptide and a fragment associated with the remaining $\text{Arg}^1\text{-Pro}^2$ dipeptide (discussed in detail below). This pair forms upon cleavage of $\text{Pro}^2\text{-Pro}^3$, which as noted above is enzymatically resistant. By ~ 150 min, the $[\text{BK}_{(3,9)}+2\text{H}]^{2+}$ and $\text{Arg}^1\text{-Pro}^2$ fragments dominate the mass spectrum, and are the only species observed beyond ~ 300 min. These data indicate that $[\text{BK}+2\text{H}]^{2+}$ is converted to $[\text{BK}+3\text{H}]^{3+}$ through a slow protonation reaction, and that the triply protonated peptide undergoes a cleavage of the $\text{Pro}^2\text{-Pro}^3$ peptide bond. This transformation is remarkably selective, ultimately forming the seven residue $[\text{BK}_{(3,9)}+2\text{H}]^{2+}$ product with $\sim 100\%$ efficiency.

Of immediate interest is the slow protonation reaction. Such a slow transfer of a proton, the lightest and fastest chemical moiety, suggests that a key barrier must regulate protonation. A clue about this barrier comes from a recent study of polyproline-7 showing that a cooperative *cis* \rightarrow *trans* isomerization of all peptide bonds was responsible for regulating the slowest proton transfer reaction ever measured.¹⁷ The slow protonation event observed here suggests a similar configurational change may regulate this system.

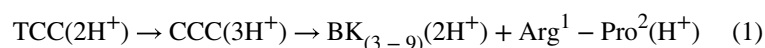
This structural transition can be directly tested for BK by examining IMS cross section distributions shown in Figure 2. The mobility of an ion through a buffer gas, under the influence of a weak field, depends on its collision cross section with the buffer gas.^{18–21} Structures having different cross sections arise from different combinations of *cis*- and *trans*-configurations of Pro^2 , Pro^3 , and Pro^7 residues, which have been characterized previously by IMS-MS,¹² and recently confirmed by cryogenic IR spectroscopy.²² For $[\text{BK}+2\text{H}]^{2+}$, there are two experimentally resolved structures: a small peak, representing $\sim 5\%$ of the population at $\Omega = 240 \text{ \AA}^2$ and a more abundant species having $\Omega = 244 \text{ \AA}^2$. The configurations of the three proline residues in these structures have been assigned as *trans*- Pro^2 , *trans*- Pro^3 , and *cis*- Pro^7 [TTC(2H⁺)] for $\Omega = 240 \text{ \AA}^2$; and, *trans*- Pro^2 , *cis*- Pro^3 , *cis*- Pro^7 [TCC(2H⁺)] for $\Omega = 244 \text{ \AA}^2$ (see Supporting Information). Four conformations resolved for $[\text{BK}+3\text{H}]^{3+}$ are assigned to the following proline configurations: the largest peak at $\Omega = 269 \text{ \AA}^2$, corresponds to [CCC(3H⁺)];¹² a peak at $\Omega = 278 \text{ \AA}^2$, in which the *cis/trans* configurations have not been assigned is designated as [B'(3H⁺)]; a low-abundance species at $\Omega = 285 \text{ \AA}^2$ as [CTT(3H⁺)];^{12,22} and, the small peak at $\Omega = 306 \text{ \AA}^2$ as [TTC(3H⁺)].¹² Figure 2 shows that upon initiation of these cross section measurements, the TCC(2H⁺) configuration is most abundant. As the reaction progresses (~ 75 min) the fraction of TCC(2H⁺) decreases and there is a corresponding increase in the abundance of triply protonated BK in the CCC(3H⁺) form. This indicates that, as was observed for Pro_7 ,¹⁷ the slow-protonation event is regulated by a conformational change; in the case of BK, the *trans* \rightarrow *cis* conversion of the $\text{Arg}^1\text{-Pro}^2$ peptide bond [i.e., the doubly protonated TCC(2H⁺) conformation] is converted to the triply protonated all-*cis* CCC(3H⁺) conformation. In this way, the configuration of $\text{Arg}^1\text{-Pro}^2$ regulates the rate of the proton transfer event. This configurational change must allow access to an additional basic site that is preferentially protonated.

Two immediate questions emerge. How does $\text{Pro}^2\text{-Pro}^3$ cleavage occur? And, why would the intrinsically most-favored process be avoided biologically? To understand how Pro-Pro bond

cleavage occurs in the absence of enzymes we need to understand the reaction mechanism. We begin by noting that the Arg¹-Pro² fragment lacks a C-terminal carboxylic acid moiety and thus likely exists as the well-known cyclized diketopiperazine (DKP) structure of Arg¹-Pro².²³ The Arg¹-Pro² DKP species is formed when the N-terminus is in close proximity to the carbonyl carbon between the second and third residues. Scheme 1 illustrates a simple mechanism of formation arising from nucleophilic attack of the amino terminus on the carbonyl carbon atom,²³ a process that cleaves the C—N peptide bond, yielding the cyclic Arg¹-Pro² DKP, and the linear seven-residue peptide (Pro³-Gly⁴-Phe⁵-Ser⁶-Pro⁷-Phe⁸-Arg⁹). Previous studies of a C-terminally amidated Ala-Pro-NH₂ dipeptide reported an overall reaction rate that is also limited by the *trans* → *cis* isomerization of the Ala-Pro peptide bond,²³ analogous to results reported here, and further corroborating our *cis/trans* configurational assignments. It is worth noting that this mechanism does not require the additional protonation event. Thus, the role of the third proton remains somewhat unclear; this change may be off pathway and unassociated with bond cleavage.

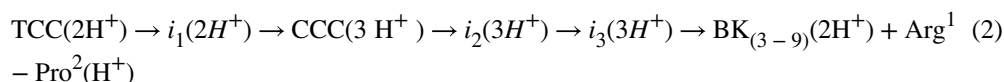
Insight about how this occurs can be gleaned by modeling the experimental kinetics data shown in Figure 3. This approach provides insights about the details of reaction pathways.^{24,25} We first assume a model reaction pathway and then write differential rate equations for the assumed process. Upon solving the system of differential equations at all times and optimizing this solution with respect to the experiment, we obtain kinetics curves for the model pathway that can be compared with the experiment.

Consider the model pathway shown by reaction 1:



this is the simplest model that includes the experimentally resolved intermediate [i.e., formation of CCC(3H⁺)]. Optimization of this model yields values of $k_1 = 7.5 \times 10^{-3} \text{ s}^{-1}$ for formation of CCC(3H⁺) and $k_2 = 1.4 \times 10^{-2} \text{ s}^{-1}$ for depletion of CCC(3H⁺) and formation of the product fragments at 65 °C. Dashed lines in Figure 3 represent this model pathway. Although this model captures the general shapes of the experimental kinetics curves, it unfortunately misses some key points. For example, experimental data shows that the TCC(2H⁺) → CCC(3H⁺) step is observed after a ~10 min induction period: the resulting shape is not captured by the single-intermediate decay process.

Fortunately, it is possible to calculate many different trial models. We have tested 34 possible model pathways (see Supporting Information). A representation of the quality of each of these processes (that include up to five intermediates and consider sequential and parallel pathways) is shown in Figure 3 as a residual sum of squares plot. From this analysis, we find that the best representation of experiment comes from a model pathway that includes a hidden intermediate²⁴ associated with *trans* → *cis* isomerization of Arg¹-Pro² [i.e., TCC(2H⁺) → $i_1(2H^+) \rightarrow \text{CCC}(3H^+)$], and two additional intermediates associated with bond cleavage [i.e., CCC(3H⁺) → $i_2(3H^+) \rightarrow i_3(3H^+) \rightarrow \text{BK}_{(3,9)}(2H^+) + \text{Arg}^1 - \text{Pro}^2(\text{H}^+)$], leading to the complete process, reaction 2.



Though the structures of these intermediates remain entirely uncharacterized, evidence for their existence from this analysis is remarkable, as it suggests a minimum number of large barriers (five) associated with spontaneous dissociation of BK. Thus, we note that although this process is spontaneous, it is not easy. Measurements and analysis of these kinetics at different solution temperatures ($T = 55, 60, 65, 70, 75,$ and 78 °C) can be used to obtain Arrhenius plots (see Supporting Information), and from transition state theory we can estimate step-by-step thermochemistry associated with each of these barriers. This analysis for our best pathway (i.e., reaction 2) yields transition state free energies of $G^\ddagger = 93.1 \pm 12.1, 94.8 \pm 0.2, 94.0 \pm 9.1, 93.9 \pm 9.7,$ and 94.1 ± 9.2 kJ·mol⁻¹ for each sequential step as reaction 2 progresses. When we partition the free energies into enthalpic (H^\ddagger) and entropic (S^\ddagger) terms, we find that the contributions of H^\ddagger to the barriers for the two steps $\text{TCC}(2\text{H}^+) \rightarrow i_1(2\text{H}^+) \rightarrow \text{CCC}(3\text{H}^+)$ are 97.7 ± 12.1 kJ·mol⁻¹ and 79.8 ± 1.6 kJ·mol⁻¹, respectively. For the three steps after isomerization, which lead to dissociation [i.e., $\text{CCC}(3\text{H}^+) \rightarrow i_2(3\text{H}^+) \rightarrow i_3(3\text{H}^+) \rightarrow \text{BK}_{(3-9)}(2\text{H}^+) + \text{Arg}^1 - \text{Pro}^2(\text{H}^+)$], we obtain $H^\ddagger = 105.8 \pm 9.1, 106.7 \pm 9.7,$ and 107.3 ± 9.2 kJ·mol⁻¹, respectively. The corresponding entropic components of each step shows that a late step associated with *trans* \rightarrow *cis* isomerization of the Arg¹-Pro² bond involves a tight, entropically restricted transition state [$S^\ddagger = 15.3 \pm 2.5$ J·K⁻¹·mol⁻¹ for the first $\text{TCC}(2\text{H}^+) \rightarrow i_1(2\text{H}^+)$ step and -50.4 ± 1.7 J·mol⁻¹·K⁻¹ for the later $i_1(2\text{H}^+) \rightarrow \text{CCC}(3\text{H}^+)$ transition]. The entropic contributions to the three barriers associated with the $\text{CCC}(3\text{H}^+) \rightarrow i_2(3\text{H}^+) \rightarrow i_3(3\text{H}^+) \rightarrow \text{BK}_{(3-9)}(2\text{H}^+) + \text{Arg}^1 - \text{Pro}^2(\text{H}^+)$ rearrangements and bond cleavage shows that each step proceeds through a relatively loose (entropically allowed) transition state (i.e., $S^\ddagger = 39.4 \pm 4.6, 42.8 \pm 5.2,$ and 44.4 ± 5.1 J·mol⁻¹·K⁻¹, respectively, for sequential steps leading to bond cleavage).

With this understanding about how spontaneous Pro²-Pro³ dissociation occurs in the absence of enzymes, we turn our attention to the question of why would the most intrinsically favored process be avoided biologically? Our finding, that cleavage between Pro²-Pro³ is the only accessible pathway spontaneously, is remarkable considering that this bond is not processed enzymatically. It turns out that the seven-residue BK₍₃₋₉₎ is nearly an order of magnitude more antigenic than the BK nonapeptide as well as the eight-residue BK₍₂₋₉₎ peptide.²⁶ Rather than form BK₍₃₋₉₎ enzymatically, BK can be processed by aminopeptidase P to form the eight-residue peptide (which lacks typical BK activity), followed by DPP-IV elimination of Pro²-Pro³, thus avoiding the antigenic repercussions associated with BK₍₃₋₉₎ formation.

Finally, it is important that while spontaneous Pro²-Pro³ cleavage is favored intrinsically, this processing is slow. Biologically, the deleterious antigenic impact of spontaneous cleavage is avoided by rapid enzymatic degradation of the Arg¹-*trans*-Pro² configured BK. Structural studies of penultimate proline containing peptides interacting with the DPP-IV enzyme show that the *trans*-Pro²-peptide is the bound form which leads to enzyme cleavage,

²⁷ consistent with this idea. In this way, the biological processing mechanism naturally regulates antigenicity, as enzymatic degradation of BK leads to inactive species^{7,28}.

Supplementary Material

Refer to Web version on PubMed Central for supplementary material.

ACKNOWLEDGMENTS

This work is supported in part by funds from the National Institutes of Health, R01 GM117207-03, the Indiana University Robert and Marjorie Mann endowment fellowship (C.R.C.), and a fellowship from the Indiana University College of Arts and Sciences (T.J.E.-B.).

REFERENCES

- (1). Benesch JL; Sobott F; Robinson CV *Anal. Chem.* 2003, 75, 2208–2214. [PubMed: 12918957]
- (2). Wang G; Abzalimov RR; Kaltashov IA *Anal. Chem.* 2011, 83, 2870–2876. [PubMed: 21417416]
- (3). Cong X; Liu Y; Liu W; Liang X; Russell DH; Laganowsky AJ *Am. Chem. Soc.* 2016, 138, 4346–4349.
- (4). El-Baba TJ; Woodall DW; Raab SA; Fuller DR; Laganowsky A; Russell DH; Clemmer DE J. *Am. Chem. Soc.* 2017, 139, 6306–6309. [PubMed: 28427262]
- (5). Vanhoof G; Goossens F; De Meester I; Hendriks D; Scharpe S *FASEB J.* 1995, 9, 736–744. [PubMed: 7601338]
- (6). Abelous J; Bardier EC *R. Soc. Biol.* 1909, 66, 511–512.
- (7). Regoli D; Barabe J *Pharmacol. Rev.* 1980, 32, 1–46. [PubMed: 7015371]
- (8). Dray A; Perkins M *Trends Neurosci.* 1993, 16, 99–104. [PubMed: 7681240]
- (9). Basbaum AI; Bautista DM; Scherrer G; Julius D *Cell* 2009, 139, 267–284. [PubMed: 19837031]
- (10). Pierson NA; Chen L; Valentine SJ; Russell DH; Clemmer DE J. *Am. Chem. Soc.* 2011, 133, 13810–13813. [PubMed: 21830821]
- (11). Young JK; Hicks RP *Biopolymers* 1994, 34, 611–623. [PubMed: 8003621]
- (12). Pierson NA; Chen L; Russell DH; Clemmer DE J. *Am. Chem. Soc.* 2013, 135, 3186–3192. [PubMed: 23373819]
- (13). Denys L; Bothner-By A; Fisher G *Biochemistry* 1982, 21, 6531–6536. [PubMed: 7150573]
- (14). Lopez JJ; Shukla AK; Reinhart C; Schwalbe H; Michel H; Glaubitz C *Angew. Chem.* 2008, 120, 1692–1695.
- (15). Merenbloom SI; Koeniger SL; Valentine SJ; Plasencia MD; Clemmer DE *Anal. Chem.* 2006, 78, 2802–2809. [PubMed: 16615796]
- (16). Koeniger SL; Merenbloom SI; Valentine SJ; Jarrold MF; Udseth HR; Smith RD; Clemmer DE *Anal. Chem.* 2006, 78, 4161–4174. [PubMed: 16771547]
- (17). Shi L; Holliday AE; Khanal N; Russell DH; Clemmer DE J. *Am. Chem. Soc.* 2015, 137, 8680–8683. [PubMed: 26115587]
- (18). Mason EA; McDaniel EW *Transport properties of ions in gases*; Wiley: New York, NY, 1988.
- (19). Von Helden G; Hsu MT; Kemper PR; Bowers MT *J. Chem. Phys.* 1991, 95, 3835–3837.
- (20). Jarrold MF; Constant VA *Phys. Rev. Lett* 1991, 67, 2994–2997. [PubMed: 10044611]
- (21). Clemmer DE; Jarrold MF *J. Mass Spectrom.* 1997, 32, 577–592.
- (22). Voronina L; Scutelnic V; Masellis C; Rizzo TR *J. Am. Chem. Soc.* 2018, 140, 2401–2404. [PubMed: 29412650]
- (23). Capasso S; Vergara A; Mazzarella LJ *Am. Chem. Soc.* 1998, 120, 1990–1995.
- (24). El-Baba TJ; Kim D; Rogers DB; Khan FA; Hales DA; Russell DH; Clemmer DE J. *Phys. Chem. B* 2016, 120, 12040–12046. [PubMed: 27933943]
- (25). Shi L; Holliday AE; Shi H; Zhu F; Ewing MA; Russell DH; Clemmer DE J. *Am. Chem. Soc.* 2014, 136, 12702–12711. [PubMed: 25105554]

- (26). Redman L; Regoli D; Tustanoff ER Can. J. Biochem. 1979, 57, 529–539. [PubMed: 476504]
- (27). Fischer G; Heins J; Barth A Biochim. Biophys. Acta, Protein Struct. Mol. Enzymol 1983, 742, 452–462.
- (28). Kuoppala A; Lindstedt KA; Saarinen J; Kovanen PT; Kokkonen JO Am. J. Physiol.: Heart Circ. Physiol. 2000, 278, H1069–H1074. [PubMed: 10749699]

Author Manuscript

Author Manuscript

Author Manuscript

Author Manuscript

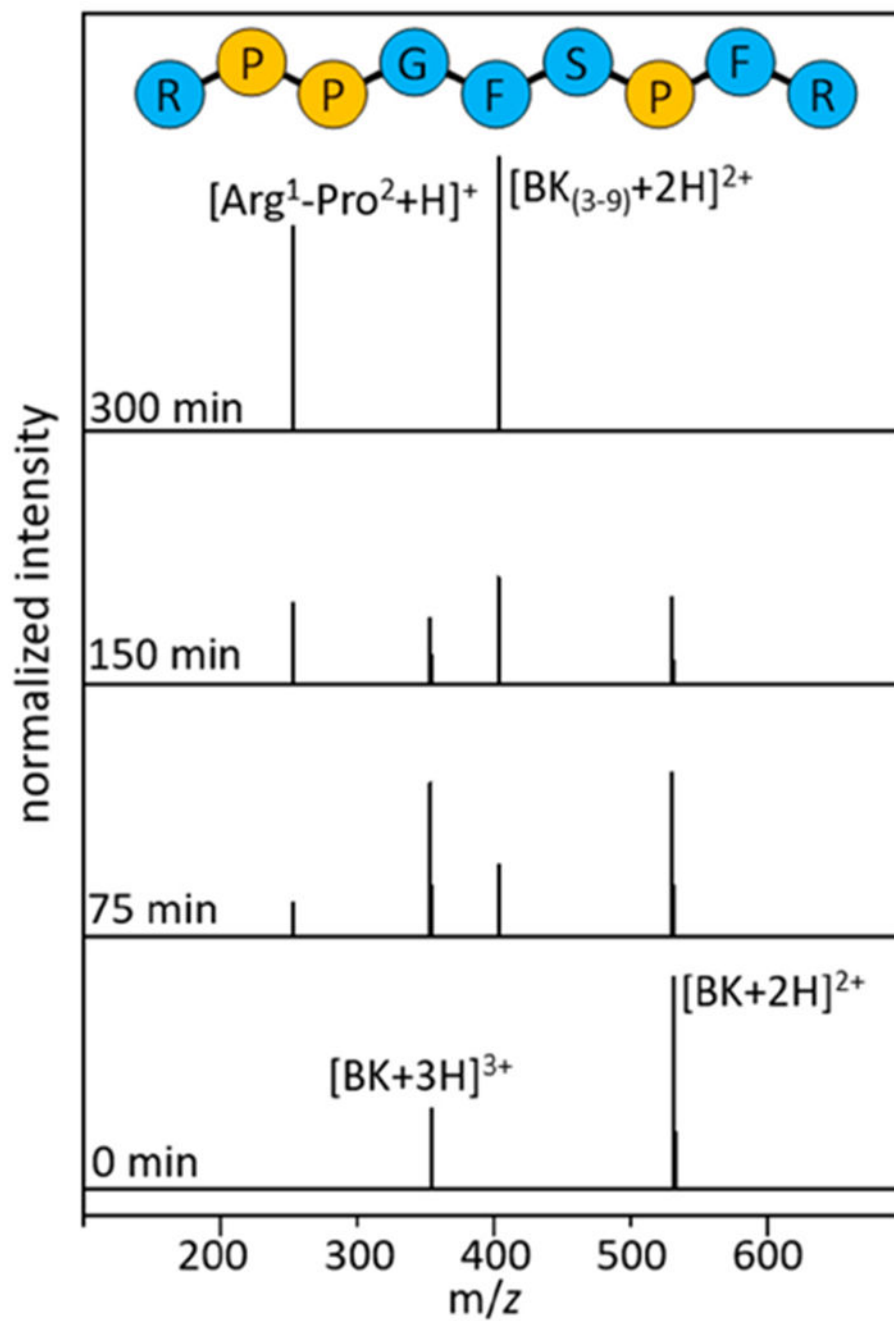


Figure 1.
Mass spectral distributions shown at 0, 75, 150, and 300 min.

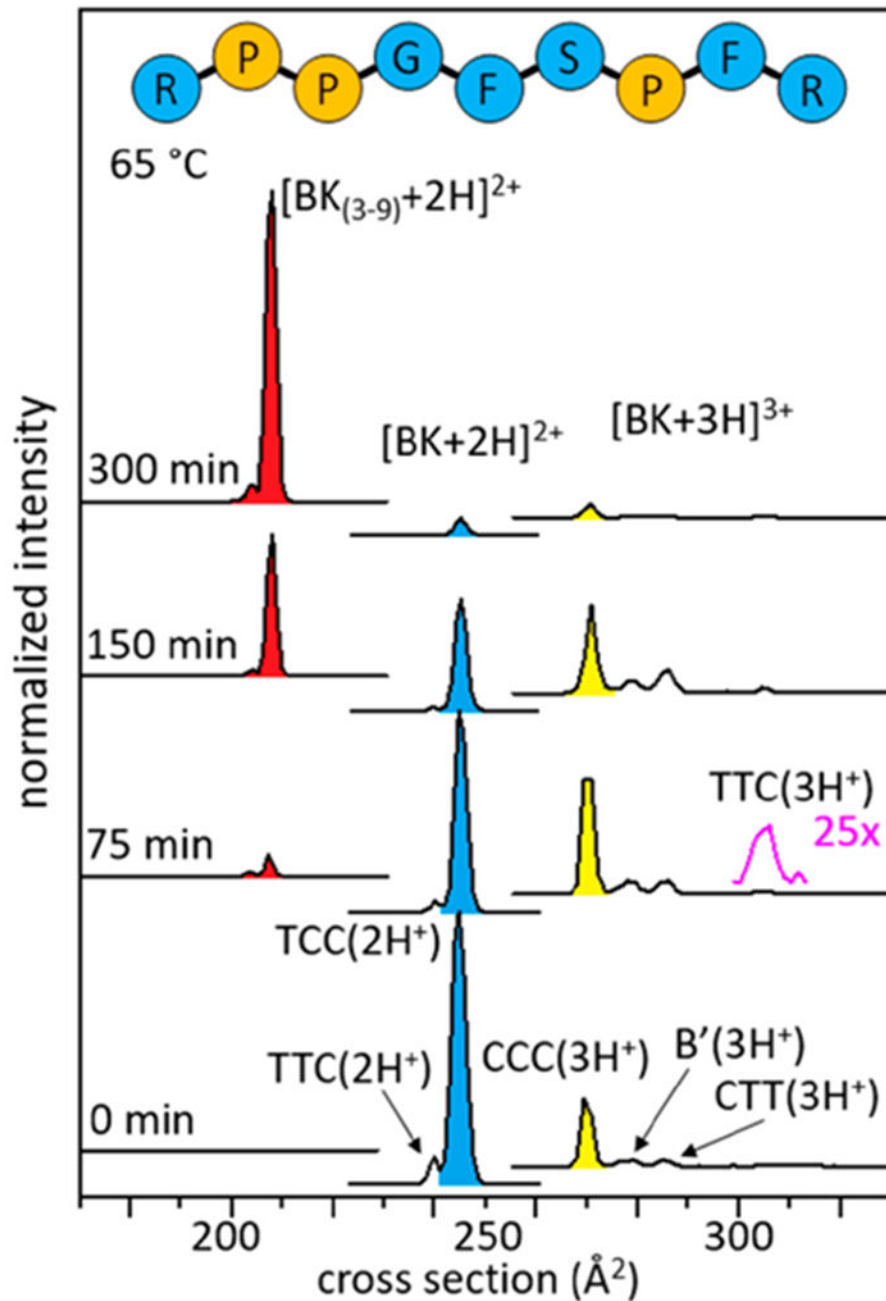


Figure 2. Cross section distributions shown at 0, 75, 150, and 300 min. The blue peak represents the TCC(2H⁺) configuration, the yellow peak represents CCC(3H⁺), and the red peak represents [BK(3-9)+2H]²⁺, which are the most abundant conformations in the IMS-MS distributions. The cross section for Arg¹-Pro² (not shown in the figure) is $\Omega = 96 \text{ \AA}^2$.

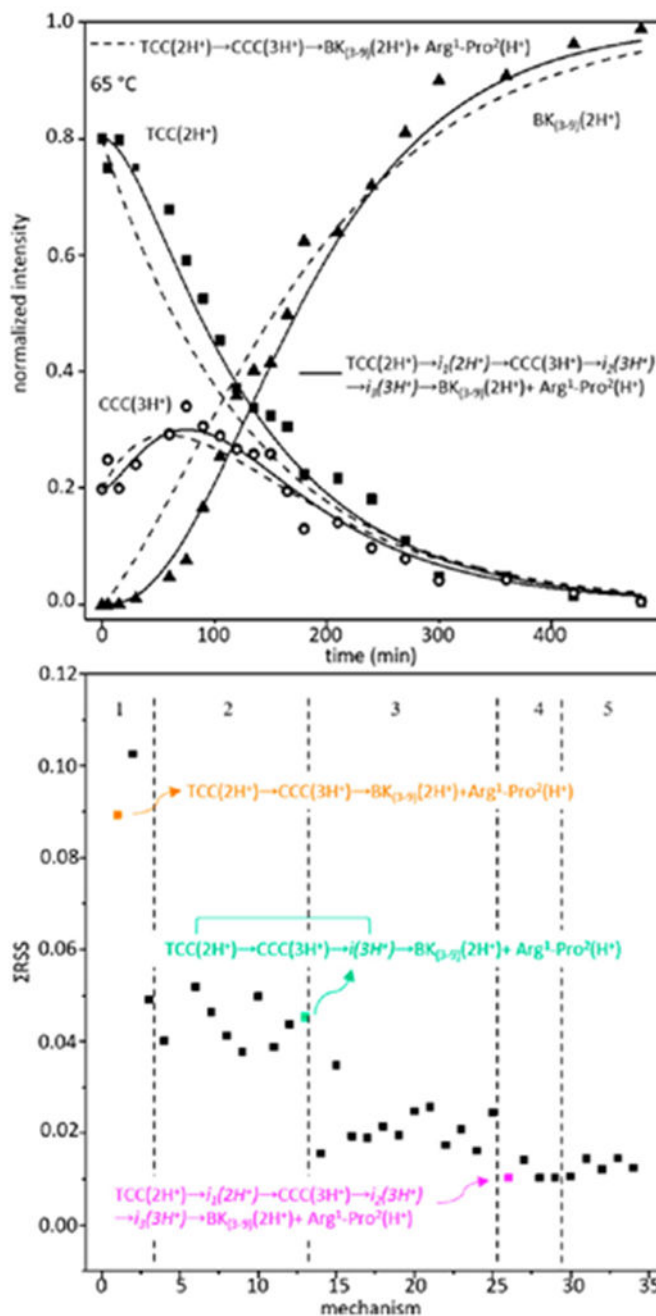
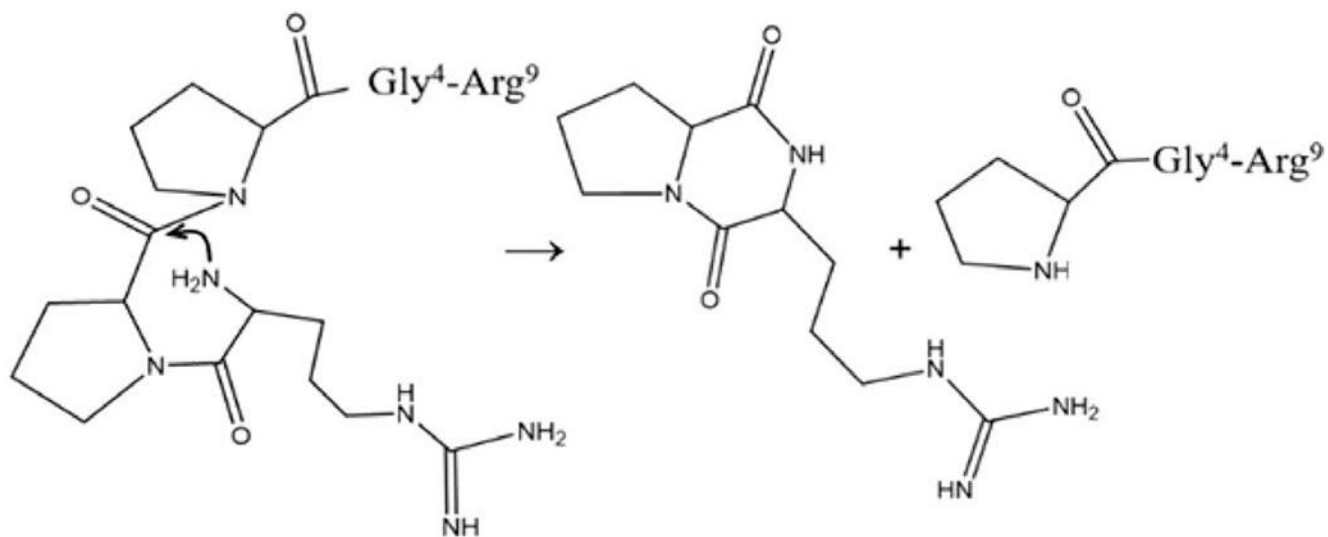


Figure 3.

Kinetics data shown at 65 °C (top). Two models are shown with the solid line representing $\text{TCC}(2\text{H}^+) \rightarrow i_1(2\text{H}^+) \rightarrow \text{CCC}(3\text{H}^+) \rightarrow i_2(3\text{H}^+) \rightarrow i_3(3\text{H}^+) \rightarrow \text{BK}(3-9)(2\text{H}^+) + \text{Arg}^1\text{-Pro}^2(\text{H}^+)$, among the statistically best models, and the dashed line representing $\text{TCC}(2\text{H}^+) \rightarrow \text{CCC}(3\text{H}^+) \rightarrow \text{BK}(3-9)(2\text{H}^+) + \text{Arg}^1\text{-Pro}^2(\text{H}^+)$, the simplest model. Bottom panel shows residual sums of squares values for each model, separated by dashed lines corresponding to 1-5 intermediates. Three example reaction pathways are shown.

**Scheme 1.**

Cleavage mechanism of Pro²-Pro³ by DKP formation with Arg¹-Pro² in the cis configuration